Swift Diagnose: A High-Performance Shallow Convolutional Neural Network for Rapid and Reliable SARS-COV-2 Induced Pneumonia Detection

Koustav Dutta[1], Rasmita Lenka[2], Priya Gupta[3*], Aarti Goel[4] and Janjhyam Venkata Naga Ramesh[5]

[1]SA&MA: Analytics & Cognitive, Deloitte Touche Tohmatsu India LLP
[2]School of Electronics Engineering, KIIT Deemed to be University, India
[3]Atal Bihari Vajpayee School of Management and Entrepreneurship, Jawaharlal Nehru University, New Delhi, India
[4]Hansraj College, University of Delhi, New Delhi, India
[5]Department of Computer Science and Engineering, Koneru Lakshmaiah Education Foundation, Vaddeswaram, Guntur Dist., Andhra Pradesh - 522302, India

Abstract

INTRODUCTION: The SARS-COV-2 pandemic has led to a significant increase in the number of infected individuals and a considerable loss of lives. Identifying SARS-COV-2-induced pneumonia cases promptly is crucial for controlling the virus's spread and improving patient care. In this context, chest X-ray imaging has become an essential tool for detecting pneumonia caused by the novel coronavirus.

OBJECTIVES: The primary goal of this research is to differentiate between pneumonia cases induced specifically by the SARS-COV-2 virus and other types of pneumonia or healthy cases. This distinction is vital for the effective treatment and isolation of affected patients.

METHODS: A streamlined stacked Convolutional Neural Network (CNN) architecture was employed for this study. The dataset, meticulously curated from Johns Hopkins University's medical database, comprised 2292 chest X-ray images. This included 542 images of COVID-19-infected cases and 1266 non-COVID cases for the training phase, and 167 COVID-infected images plus 317 non-COVID images for the testing phase. The CNN's performance was assessed against a well-established CNN model to ensure the reliability of the findings.

RESULTS: The proposed CNN model demonstrated exceptional accuracy, with an overall accuracy rate of 98.96%. In particular, the model achieved a per-class accuracy of 99.405% for detecting SARS-COV-2-infected cases and 98.73% for identifying non-COVID cases. These results indicate the model's significant potential in distinguishing between COVID-19-related pneumonia and other conditions.

CONCLUSION: The research validates the efficacy of using a specialized CNN architecture for the rapid and precise identification of SARS-COV-2-induced pneumonia from chest X-ray images. The high accuracy rates suggest that this method could be a valuable tool in the ongoing fight against the COVID-19 pandemic, aiding in the swift diagnosis and effective treatment of patients.

*Corresponding author. Email: priyagupta@jnu.ac.in

1. Introduction

The COVID-19 pandemic had a profound global impact, resulting in significant loss of life and affecting millions of people worldwide. Despite the availability of vaccines to mitigate the virus's spread and severity, practical strategies for diagnosis and containment remain critical. Accurate identification of infected cases was essential for preventing further transmission and managing outbreaks efficiently. While vaccines have provided a crucial tool in the fight

against SARS-COV-2, diagnostic methods continue to play a vital role in pandemic management. Various diagnostic procedures, including molecular, antigen, and antibody tests, are commonly employed to detect and monitor the disease. Molecular tests offer high accuracy but often have longer turnaround times.

In contrast, antigen and antibody tests provide faster results but may have higher rates of false negatives. SARS-COV-2 symptoms may vary from mild to severe, with severe cases potentially leading to pneumonia. Understanding the disease's incubation period and progression remains crucial.

While vaccines are a crucial tool in pandemic management, diagnostic methods remain essential, particularly for identifying new variants, managing breakthrough infections, and ensuring timely medical care. Over eight lakh people have died from SARS-CoV-2 infections, affecting more than 24 million people worldwide. Because it is incredibly contagious, contact tracing and detection are the only effective control methods. Since no vaccine is currently in development, the only option is to precisely identify and isolate infected cases to halt the spread of illnesses. Molecular testing, antigen tests, and antibody tests are used to detect disease in general. Though the Molecular test is exact, it is time-consuming as it may take days for the result to come. While the Antigen and Antibody tests take less time, the false-negative results rate is higher [1][2]. SARS-COV-2 symptoms often mimic the seasonal flu, including cough, myalgia, throat pain, headache, fever, and other flu-like symptoms. It can lead to breathing difficulties in severe cases, especially in individuals with comorbidities or compromised immune systems [3]. When the infection reaches the lungs, it can result in SARS-COV-2-induced pneumonia, requiring immediate medical attention. Coronaviruses are a group of RNA viruses that primarily infect animals and birds but can also infect humans, causing respiratory tract infections. The severity of the pandemic varies, with around 80% of cases being mild, 13% severe, and 6% critical. Adhering to government guidelines is crucial to fighting the virus [31]. During the monsoon season, seasonal flu and pneumonia, often caused by viruses, become prevalent in many developing countries like India, putting additional strain on fragile healthcare infrastructures. Chest X-rays, a commonly used diagnostic tool, can potentially serve as a first-line method for detecting and diagnosing SARS-COV-2-induced pneumonia, particularly in regions with limited testing access (NCIP). This approach can help distinguish between the symptoms of pneumonia resulting from viral infections like SARS-COV-2 and those caused by the seasonal flu.

Even with the availability of vaccines, the need for effective prediction and diagnosis methods persists. Early detection and accurate diagnosis remain critical in regions with prevalent seasonal flu and other respiratory illnesses. These methods can help identify breakthrough cases in vaccinated individuals, monitor virus mutations, and guide appropriate medical interventions. While vaccines have significantly reduced the severity of SARS-COV-2 cases and curbed the spread, ongoing research explores various computational techniques to predict and manage the pandemic. Forecasting models continue to assess mortality rates and associated risks, with machine learning and deep learning models playing a pivotal role in diagnosing SARS-COV-2 and differentiating it from other respiratory conditions.

Intelligent prediction and diagnosis techniques are highly desirable because early detection can help contain the virus's spread and ensure appropriate medical care. Various computational methods, including deep learning, machine learning, mathematics, and statistical approaches, have been employed successfully to predict and monitor the SARS-COV-2 pandemic [4][5][34][35]. These approaches include forecasting models to assess mortality rates and associated risks. Researchers have used these models to predict SARS-COV-2 cases efficiently, even with limited data [26][33]. Additionally, deep learning models have played a vital role in diagnosing SARS-COV-2 and distinguishing it from other respiratory conditions [30][32]. Artificial intelligence (AI) systems, including the Multi-Scale Convolutional Neural Networks (MSCNN), have found utility in analyzing CT scans from SARS-CoV-2 patients. These AI algorithms exhibit promising diagnostic capabilities in recognizing SARS-CoV-2 infections and distinguishing them from other forms of pneumonia, achieving a notably high recall rate of 99.39%. What distinguishes this Lightweight Stacked Convolutional Neural Network Architecture from others is its remarkable reduction in time complexity and memory demands. It attains impressive accuracy levels while employing significantly fewer parameters, thereby enhancing efficiency [6][28][29][30].

While introducing vaccines has reshaped the battle against SARS-CoV-2, the significance of precise diagnostic and predictive methods remains unwavering. These methodologies are crucial in ongoing efforts to manage the pandemic, adapt to emerging challenges, and identify novel variants. The Lightweight Stacked Convolutional Neural Network Architecture proposed in this research paper represents a promising stride forward in SARS-CoV-2 diagnosis, offering a highly efficient and accurate tool for the detection and ongoing monitoring of the disease.

In this context, incorporating machine learning and deep learning models [7][8], such as the one presented in this research, remains invaluable. These models complement vaccination initiatives by providing efficient diagnostic and monitoring capabilities, ensuring a comprehensive approach to tackling the pandemic.

2. Research Design

This section will explore the dataset employed in this research and the fundamental meth-odology that drives our approach. This section is structured into two primary subsections: the first section addresses the dataset utilized in our methods, while the subsequent part elucidates the central concept underpinning our model.

2.1. Dataset Description

The dataset utilized for this study is open-sourced and is obtained from the Johns Hopkins University medical database (USA), with a corresponding dataset available at the following URL: https://github.com/education454/datasets.git. This dataset consists of chest X-ray im-ages, explicitly focusing on individuals with SARS-COV-2-induced pneumonia and those with normal chest X-ray findings. It is imperative to note that the dataset includes chest X-ray images from individuals of diverse demographic backgrounds, including varying age groups, genders, and ethnicities.

• Training Set: The training set includes X-ray images of the Chest from 545 indi-viduals infected with SARS-COV-2 and 1266 standard Chest X-ray images.

• Validation Set: The validation set comprises 167 SARS-COV-2 X-ray images of the Chest and 317 standard X-ray images of the Chest.

Figures 1.1, 1.2, and 1.3 show the images of the X-Ray of the Chest of SARS-COV-2 infected and the X-Ray of the normal Chest.
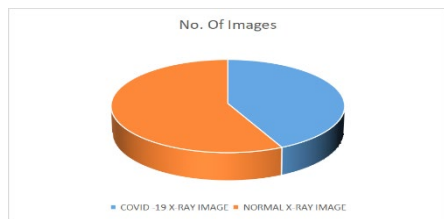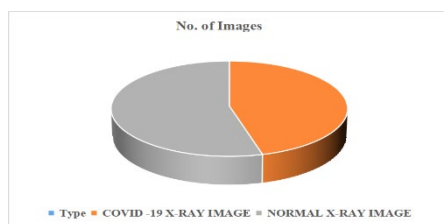

Figure 1.1: Composition of Training Data Images

Figure 1.2: Composition of Validation Data Images
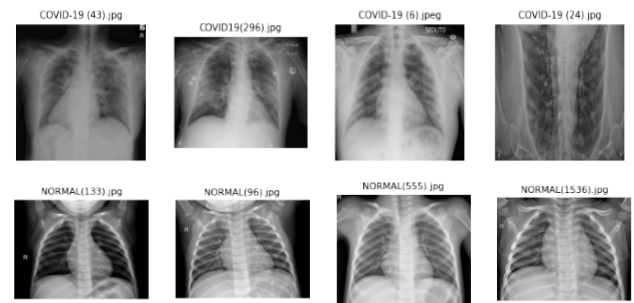

Figure 1.3: SARS-COV-2 and Normal chest X-Ray images

As observed from the dataset, a significant data imbalance exists, with more standard chest X-ray images than SARS-COV-2-induced pneumonia cases. Such data imbalance can pose challenges during model training and evaluation, potentially leading to biases in the model's performance. To mitigate this issue, a data balancing strategy has been employed to ensure that the model is exposed to nearly equal amounts of data from each class during training. To ensure accurate detection, an Image data augmentation approach has been employed.

Image data augmentation [9] serves as a technique employed to artificially expand the size of a training dataset by generating modified versions of the images contained within the dataset.

This augmentation process enriches the training data, ultimately enhancing the capabilities of deep-learning neural network models. By introducing various transformations to the images, such as shifts, flips, zooms, and other operations, this approach aims to present a more comprehensive array of potential patterns in the training dataset. These variations represent diverse instances of the training set images that the model is expected to encounter. In this research, image augmentation is achieved by applying a 20 percent zoom in and out on the images and performing horizontal flips on the dataset images.

2.2 Proposed Algorithm and Architecture

This study presents a practical methodology for analyzing and detecting COVID-19 in chest X-rays. A robust and lightweight stacked convolutional neural network has been developed to handle datasets of varying sizes and contend with noise. This innovation addresses a common challenge conventional methods face and ensures the most precise detection possible, boasting an impressive overall average accuracy rate of 98.76%. What sets this approach apart is its shallow time complexity, requiring only 240 milliseconds for execution, and its minimal memory footprint, resulting in an exceptionally efficient algorithmic process. Below, we provide an overview of the Stacked Convolutional Neural Network layers and elucidate their functions.

2.2.1 Stacked Convolutional Neural Network (CNN)

The Stacked Convolutional Neural Network comprises various essential layers, including Convolution Layers, Pooling Layers, Dropout Layers, Flattening Layers, and Fully Connect-ed Layers. For image processing tasks, Convolutional Neural Networks (CNNs) represent a robust deep-learning framework [10]. In our system, the entire foundation is constructed using a CNN. CNNs, such as the one illustrated [11], exemplify deep learning techniques capable of discerning images by extracting meaningful features, a pivotal aspect in comput-er vision applications and fine-tuning. This multi-layer perceptron-based architecture is employed in tasks like image classification, image segmentation, and object detection, pre-senting valuable applications in fields such as robotic vision and autonomous drone control. CNNs, with their deep learning capabilities, have also found a niche in the healthcare indus-try.

CNN Architecture Components: A CNN comprises two fundamental components. First, a convolution layer aids in extracting diverse features and intricate details from the input image. Second, a fully connected layer utilizes the convolution layer's insights to make precise predictions regarding the image's characteristics, often producing a vector of proba-bility scores indicating the likelihood of certain attributes belonging to specific classes. The design and functioning of a Basic Convolutional Neural Network draw inspiration from the organizational patterns of neurons in the human brain's visual cortex.

Within a CNN, neurons are organized in a three-dimensional structure, with each set of neurons analysing small patches or fragments of the input image. These groups of neurons specialize in extracting specific image features, assisting in identifying patterns. The CNN employs a sequence of layers to produce a final output, represented as a vector of probabil-ity scores, indicating the likelihood of specific attributes belonging to classes.

Key CNN Layers

- The fully connected input layer establishes connections between individual neurons and the deeper, concealed layers of the neural network. This facilitates the amal-gamation of feature extraction procedures and feature retrieval.
- Within the Convolutional Layer, feature maps are generated by applying filters that progressively scan the entire image. This process extracts a range of features, in-cluding corners and edges.
- The Pooling Layer performs feature map-down sampling, gradually diminishing the spatial dimensions of the representation. Consequently, this reduces the quantity of network parameters and computational workload.
- To mitigate overfitting, the Dropout Layer introduces a regularization technique that randomly activates and deactivates neurons.
- Data is reshaped into a one-dimensional array via the Flatten Layer, making it compat-ible with passing to subsequent layers. Typically, this layer is connected to the fi-nal classification model, often a fully connected layer.
- In a fully connected layer, feature maps are merged using weighted connections to make precise label predictions, capturing interdependencies among these features.
- The fully connected output layer generates the ultimate probability scores, aiding in identifying specific classes within the output image. Time Complexity and System Specifications: Table 1 provides an overview of time complexity and system spec-ifications. Each epoch requires 55.5 seconds, and the total training time is 27.5 minutes for execution.

Table 1: System Specifications of the work conducted.

Aspect	Specification
CPU	AMD Ryzen 5 5600X Processor
GPU	AMD Radeon RX 6700 XT
Memory	16 GB DDR4 RAM @ 3200 MHz
OS	Ubuntu 22.04 LTS, 64-bit

In Figure 2, we visually represent the arrangement and interplay of the numerous layers within the Convolutional Neural Network (CNN). The functionality and operation of each segment of this Neural Network are further elucidated through the visual aids in Figures 3, 4, 5, and 6. These figures offer a detailed insight into how each network section operates.
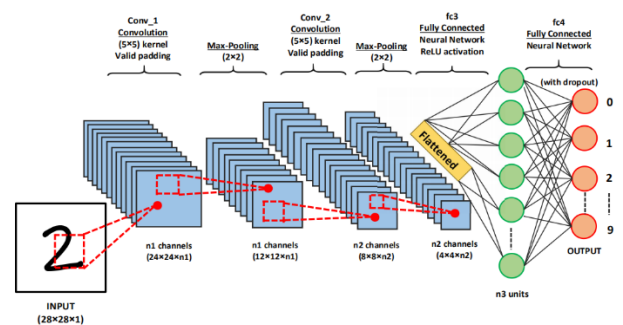

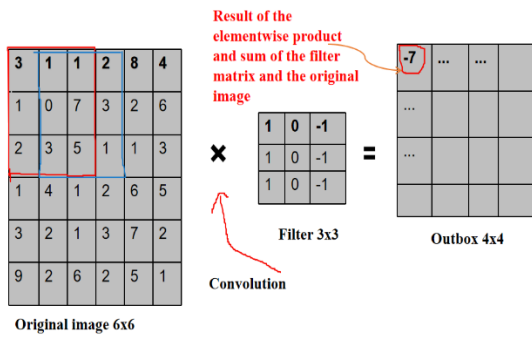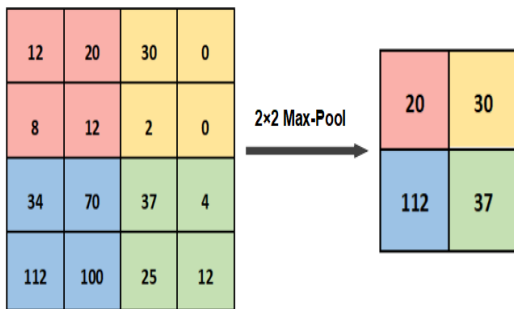**Figure.2:** Working of Convolution Neural Network

Figure. 3: Conv stratum

Figure. 4: Maximum-Pool stratum
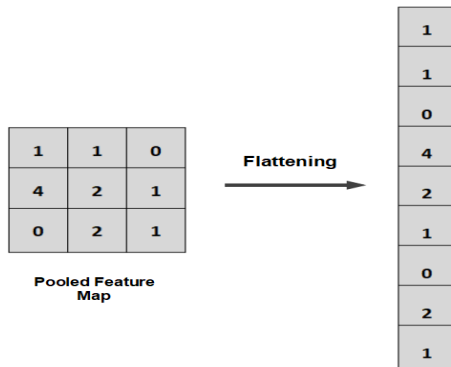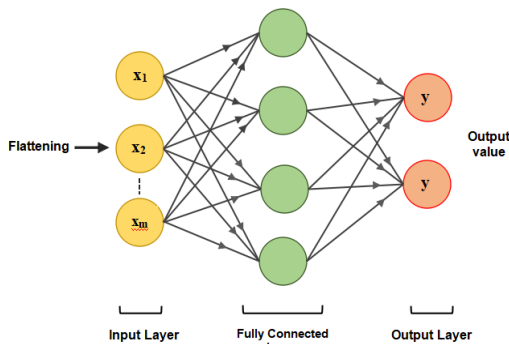

Figure. 5: Vectorization layer

Figure .6: Dense Layer and Predicted Layer

2.2.2 Suggested Lightweight Stacked CNN Structure

The Lightweight Stacked Convolutional Neural Network architecture introduced in this study is specifically designed to detect SARS-CoV-2 in chest X-ray images. This innovative architecture is tailored to process input chest X-ray images and utilizes a series of distinct layers to extract essential features necessary for accurate disease detection. The proposed model encompasses a configuration that includes two Convolutional Layers, two Max-Pooling and Dropout Layers, and culminating in Flattening and Dense Layers. These com-ponents are visually depicted in Figure 7 for clarity and understanding.
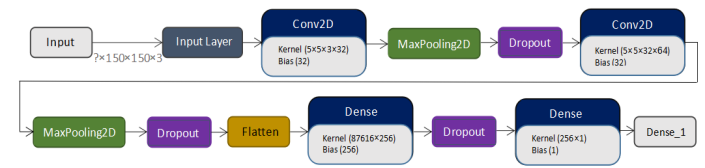

Figure 7: Diagram Depicting the Flow of the Stacked Convolutional Neural Network

When identifying SARS-CoV-2 presence in chest X-ray images and analysing standard chest X-ray images, the procedure involves inputting these X-ray images into the Light-weight Stacked Convolutional Neural Network. Within this neural network, the diverse layers are crucial in extracting intricate details and features from the chest X-ray images. This collective effort dramatically contributes to the automated detection process [12]. Here, we elucidate how these individual layers function, as well as their interplay and respective roles in the creation of feature maps:

(i) The Neural Network receives chest X-ray pictures with dimensions of $(150 \times 150 \times 3)$. The Neural Network can effectively handle any noise that the photos may have.

(ii) A Convolution Layer with 32 filters for 32 feature maps makes up the following neural network layer. For extracting the fine details & features from the input image, a (5 x 5) kernel is used as a window in this scenario. Zero Padding is also employed in these two layers to protect the data in the following layers. Additionally, each convolution layer in-corporates the L1 Regularization approach, often known as Lasso Regularization [13], al-lowing the model to learn all the hyperparameters precisely and well-defined, preventing overfitting and delivering Low Bias and Low Variance. The Activation Function used after each of the two layers is Leaky ReLU (Leaky Rectified Linear Unit) [14], which helps in extracting the non-linear features from the image.

(iii) A pooling layer makes up the third layer. In this instance, spatial down sampling is done with the help of a Max Pooling layer. This layer's kernel has a size of (2×2). The high-intensity fine details are retrieved

to create the feature maps and, thus, the Encoder portion of the network. To preserve the image's information in this instance, Zero Padding (SAME) is once again applied. After this layer, dropout regularisation is applied. It is a training tech-nique that ignores a subset of neurons chosen at random. They suddenly "disappeared." As a result, on the forward pass, their contribution to the temporary deactivation of down-stream neurons' activation is hindered. On the backward pass, weight updates are not added to the neuron. A p = 0.5 (50 percent) dropout is applied in this instance.

(iv) A Convolution Layer with 64 filters is again present in the fourth layer. In this instance, additional features from the input image, such as numerous edges, contours, texture, forms, corners, etc., are extracted using a (5 x 5) filter. To maintain the spatial information in the following layers, Zero Padding (SAME) is once more used in this layer. The L1 regularisa-tion technique is also incorporated with the two layers to reduce overfitting issues. Leaky ReLU (Leaky Rectified Linear Unit) Activation function, which helps extract the non-linear features from the image, is again used after this layer. Leaky ReLU is linear (identity) for all positive values and a small value of 0.01 for all negative values. Leaky ReLU is used re-peatedly as it does not suffer from the Vanishing Gradient problem [15].

(v) The fifth layer then employs the Max Pooling layer with a kernel size of (5 x 5) to perform additional spatial down-sampling, which aids in the extraction of the image's most crucial fine details and features, such as edge, corner, and morphological features as well as other essential features like the blur and sharpening features. After this layer, dropout regularisa-tion randomly activates and deactivates the neurons. This aids in extracting the key features and guards against overfitting issues.

(vi) The High Dimensional Feature Maps are then Vector-Space Transformed in the Flattening Layer into a One-Dimensional Vector. Next, each neuron connects to another to form a Dense Layer. This layer has 256 feature maps, which are put through non-linear operations by adding a Leaky ReLU Activation Function. After this layer, dropout p = 0.5 is employed once more to standardize the procedure.

(vii) To conclude, the output layer comprises a solitary neuron, and using a Sigmoid Activation Function determines its outcome. A sigmoid function is a numerical function with a charac-teristic "S"-shaped or sigmoid curve [16]. The sigmoid function is used since it occurs be-tween two points (0 to 1). As a result, it is suitable for models that need to predict probabil-ity as an output. This activation function has a 0.5 threshold, with a chance greater than 0.5 indicating the NORMAL case and a possibility less than 0.5 showing SARS-COV-2.

(viii) Figure 8 provides a visual representation of how the proposed lightweight stacked convolu-tional neural network functions, showcasing the interplay and operation of its diverse layers as employed in this research.

Upon obtaining the final layer's output during the training phase, a crucial step involves comparing this output with the original labelled image to determine the loss incurred. To quantify this loss, we employ the binary Cross-Entropy loss function, as delineated in Equation 1 [17]

$$H_p(q) = -\frac{1}{N}\sum_{i=1}^{N} y_i \cdot log\big(p(y_i)\big)$$
$$+ (1 - y_i) \cdot log\big(1 - p(y_i)\big) \qquad (1)$$

(ix) In this context, where "y" represents the label, and "p(y)" signifies the predicted proba-bility for a given data point, the process of back-propagation is employed. This technique is utilized to minimize the loss, aided by the Adaptive Delta Optimizer, to reach the global minimum. This iterative process makes adjustments to every element within the network's filters. Consequently, the loss diminishes gradually, ultimately leading to the attainment of an output with the highest achievable level of accuracy.

The "Adam optimization algorithm" represents an extension of the conventional sto-chastic gradient descent, and it has gained significant popularity in recent years within the realm of deep learning applications. Diederik Kingma, affiliated with OpenAI, and Jimmy Ba, from the University of Toronto, introduced the Adam model in their 2015 ICLR paper titled "Adam: A Method for Stochastic Optimization." This optimizer has emerged as a top choice among the research community for addressing non-convex optimization problems, primarily due to its enhanced computational efficiency. Furthermore, Adam's hyper-parameters possess straightforward interpretations and typically necessitate minimal tuning [18].

(x) The number of Epochs used during the training is 30. It is a measure of the number of training vectors that are used once for updating the weights. For batch training, each training sample passes through the learning algorithm together in one epoch before weights are up-dated. The value of the Learning Rate used in this neural network is 0.001. The Learning Rate parameter helps to decide the rate at which the derivative of the Loss Function of the Neural Network will reach zero and attain the Global Minima Position, thus optimizing the entire network. Mini-batch processing is used in the process for fast and efficient computa-tion in Neural networks, thus eradicating space and time complexity problems. The Batch size used for the training process is 32.

(xi) To ensure a comprehensive assessment of this Neural Network's performance, we employ the k-fold Cross-Validation Technique as an integral part of the network's training process. In this paper, the value of k is 10. Thus, through the continuous training process,

the 10-fold Cross-Validation helps to calculate the Validation accuracy apart from the training accuracy, which helps to give us a clear picture of whether the model is overfitting. The overall average Validation accuracy achieved due to the Light Weight Stacked Convolution Neural Network application is 98.96 %. The refinement of the work lies in the fact that this paper brings about a new interpreta-tion of the Convolution Neural Network Mechanism with the help of the Laws of Thermo-dynamics and the Kinetic Theory of Gases. Using the work of illustrious scientists such as Maxwell, Gibbs, and Boltzmann as a guide, Thermodynamics [19] examples and mecha-nisms of the working of the different layers of the Convolution Neural Network presented in this paper open a new dimension in the understanding of the working of Neural Net-works, which essentially optimizes the ways of thought and explanation of different neu-rons and synapses of the Neural Network. "We employed Gibbs sampling as a probabilistic technique to analyze the dataset. This method allowed us to estimate probability distribu-tions, which were instrumental in our data augmentation strategy."

"The Boltzmann equation has been extensively used in statistical mechanics. In our study, we draw parallels between the distribution of SARS-COV-2 cases and the statistical distributions described by Boltzmann's equation, which helped inform our predictive mod-eling." The Convolutional Neural Network (CNN) models employed in the research are described as an Energy-Based Model (EBM). This perspective primarily centers on gas mol-ecules within a given spatial environment striving to attain a state of minimum energy. It parallels the principles of the Kinetic Theory of Gases and the fundamental laws of Ther-modynamics, which apply universally to all particles within the cosmos. The concept is based upon attaining Zero Entropy by all the particles in the universe by minimum energy state attainment. The idea can be explained by the Boltzmann Distribution [20] for Gaseous Particles, which applies to any particle present in any space in the universe.

Likewise, the neurons within the neural network achieve a state of minimal energy through the optimization of trainable parameters employed in the network. Optimization functions are crucial in guiding them towards this minimum free energy state, which can be mathematically likened to reaching a global minimum point when the cost function (or loss function applied to the entire training dataset) reaches zero. Consequently, one can concep-tualize the world and its constituent particles within the universe as akin to a neural network, converging toward a state of maximum entropy characterized by minimum free energy.
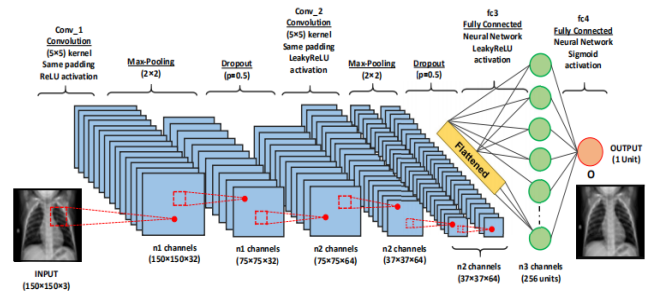

Figure. 8. Lightweight Stacked Convolutional Neural Network

3.　　Result and Discussions

This section provides a comprehensive presentation of the proposed scheme and algorithm and a detailed analysis of the results obtained. Throughout the Neural Network training process, conducted on a training set comprising 545 SARS-COV-2 cases and 1266 Normal cases, it is noteworthy that the overall average training set accuracy reached an impressive 97.54%. It's worth noting that Image Augmentation techniques have effectively addressed the challenge of data imbalance.

In the evaluation phase, the proposed Lightweight Stacked Convolutional Neural Net-work is rigorously tested against a validation set comprising 167 SARS-COV-2 cases and 317 standard cases. The overall validation accuracy is 98.96%, demonstrating the model's robust performance. Specifically, the per-class accuracy for detecting SARS-COV-2 patients is recorded at 99.405%, while the accuracy for detecting standard cases is 98.73%.

In addition to these core performance metrics, this study delves into a comprehensive exploration of alternative evaluation metrics and methodologies, providing a deeper under-standing of the suggested deep learning model's capabilities.

Since the data set is comparatively tiny, apart from using several techniques for determining the model's accuracy, the n-fold Cross-Validation technique has also been used to evaluate accuracy properly. We have considered the value of k=10 using the "Early Stopping Poli-cy." The value of accuracy, as shown above, has been achieved using this technique.

Confusion Matrix [21] has been developed for the detailed evaluation of the model from where we get to calculate the Recall Score (Sensitivity), Precision Score, and　Score. The confusion matrix, an error matrix, summarizes the model's performance in classifying instances into different categories. It consists of four key metrics:

• True Positives (TP): These are the cases where the model correctly predicted posi-tive outcomes. In our context, it refers to instances where the model

correctly identified SARS-COV-2 cases in X-ray images.

- True Negatives (TN): These are the cases where the model correctly predicted ad-verse outcomes. In our context, it refers to instances where the model correctly identified non-SARS-COV-2 cases in X-ray images.
- False Positives (FP): These are the cases where the model incorrectly predicted positive outcomes when the actual effect was negative. In our context, it refers to instances where the model incorrectly identified non-SARS-COV-2 cases as SARS-COV-2 cases in X-ray images.
- False Negatives (FN): These are the cases where the model incorrectly predicted adverse outcomes when the actual effect was positive. In our context, it refers to instances where the model incorrectly identified SARS-COV-2 cases as non-SARS-COV-2 cases in X-ray images.

Understanding these metrics is essential for evaluating the model's performance in de-tecting SARS-COV-2-induced pneumonia in chest X-ray images.

Furthermore, our examination extends to conducting an in-depth assessment of two pivotal error categories: Type 1 error and Type 2 error. The assessment outcomes, employing a range of metrics, are derived from equations denoted as 1, 2, 3, and 4 for the proposed algorithm.

$$\text{Accuracy (overall average)} = \frac{TP + TN}{TP + FP + TN + FN} \quad (2)$$

$$\text{Recall (Sensitivity)} = \frac{TP}{TP + FN} \quad (3)$$

$$\text{Precision} = \frac{TP}{TP + FP} \quad (4)$$

$$F_\beta \text{ Score} = (1 + \beta^2)\left[\frac{\text{Precision} \times \text{Recall}}{\beta^2(\text{Precision} + \text{Recall})}\right] \quad (5)$$

As the challenges addressed in this research pertain to medical contexts, the importance of the Recall metric is particularly emphasized. Consequently, we have chosen a value for the parameter β, set at 0.5, to compute the Score. This specific choice ensures that the resulting. The score must exceed two, making it a robust and meaningful evaluation metric, as outlined in Equation 6 below:

$$F_{0.5} \text{ Score} = 5\left[\frac{Precision \times Recall}{(Precision + Recall)}\right] \quad (6)$$

The number of correctly classified images of a class is TP (True Positive), the number of incorrectly classified images of a class is FP (False Positive), and the number of images of a class that have been detected as another class is FN (False Negative). The count of images that do not belong to a class and were not classified as belonging to that class is TN (True Negative) is shown in the equations. The Recall is naturally the capability of the classifier to detect all the positive samples. The best select value is 1, and the worst value is 0. The fidel-ity is intuitively the capacity of the classifier not to mark as positive a sample that is nega-tive. The F-beta Score [22] is the weighted harmonic mean of Precision and Recall, with 1 being the best and 0 being the worst. The beta parameter determines the weight of Recall in the combined score. Figure 9 illustrates the confusion matrix, while Table 2 presents the tabulated evaluation metrics.

Figure. 9: Confusion Matrix

Our findings showed that, for the decision parameters True Positives (TP), True Nega-tives (TN), False Positives (FP), and False Negatives (FN), the values were TP = 167, TN = 312, FP = 4, and FN = 1. In the context of detecting SARS-CoV-2 from chest X-ray images in our study, we use specific terms to describe the outcomes. Identifying a True Negative (TN) signifies that the model's prediction for a given chest X-ray image, labelled NORMAL, matches the input dataset, which also classifies it as NORMAL. On the other hand, a True Positive (TP) corresponds to correctly identifying a chest X-ray image as SARS-COV-2, and it was initially a case of SARS-COV-2. Interestingly, even if the original chest X-ray image was categorized as NORMAL, a False Positive (FP) indicates that the model erroneously identified it as SARS-COV-2. Lastly, a False Negative (FN) denotes instances where the model failed to place an image with NORMAL characteristics while it was initially a case of SARS-COV-2.

We derive various evaluation metrics from the Confusion Matrix, and the resulting values are presented in the Evaluation Metrics table, which includes the following indicators:

$$\text{Accuracy} = \frac{167 + 312}{167 + 312 + 1 + 4} = 0.9896 = 98.96\,\%$$

$$\text{Recall (Sensitivity)} = \frac{167}{167 + 1} = 0.9940 = 99.40\,\%$$

$$\text{Precision} = \frac{167}{167 + 4} = 0.9766 = 97.66\,\%$$

$$F_{0.5} \text{ Score} = 5 \left[\frac{0.9766 \times 0.9940}{0.9766 + 0.9940} \right] = 2.463 \quad (> 2.0)$$

$$\text{SARS-COV-2 class accuracy} = \frac{167}{167 + 1} = 0.99404 = 99.404\%$$

$$\text{NORMAL class accuracy} = \frac{312}{312 + 4} = 0.9873 = 98.73\%$$

The Recall Score is paramount in this case as it pertains to minimizing False Negative (FN) cases, aiming for the smallest possible FN value (FN = 1). This imperative underscores the necessity for a higher Recall Score than Precision, a distinction evident in the presented results. Therefore, our evaluation metrics collectively demonstrate a high degree of agreement.

From the comprehensive evaluation metrics presented in this paper, it is evident that all values align harmoniously. Specifically, the three primary evaluation parameters—Recall Score (99.40%), F0.5 score (2.463), and accuracy in classifying SARS-CoV-2 cases (99.405%)—attain the highest levels, surpassing previous works within our knowledge and literature survey.

Throughout this study, we explored various optimization functions during the algorithm's training phase to assess its effectiveness in detecting SARS-CoV-2-induced pneumonia. Additional optimization functions include Adaptive Momentum, Adaptive Gradient, Adaptive Delta, RMSProp, and Momentum-based stochastic gradient descent. Stochastic gradient descent [23] entails an iterative process for optimizing objective functions with appropriate smoothness properties, often used for high-dimensional optimization problems by replacing the actual gradient from the entire dataset with an estimate based on a randomly selected subset of data. While this approach reduces computational demands, it tends to exhibit a slower convergence rate. It is worth noting that this Optimization Algorithm, though one of the oldest and more traditional methods, yields lower accuracy than the Adam Optimizer.

On the other hand, RMSProp [24] acts as a gradient normalizer, considering the magnitude of recent gradients and dividing the current angle by a moving average over the root mean squared gradients. This optimization method yields better accuracy than the SGD Optimizer but falls slightly short of the Adam Optimizer's accuracy. The performance of these various optimization functions and the resulting overall accuracy are detailed in Table 2 for reference.

Table 2: Optimization Algorithms vs. Accuracy Score

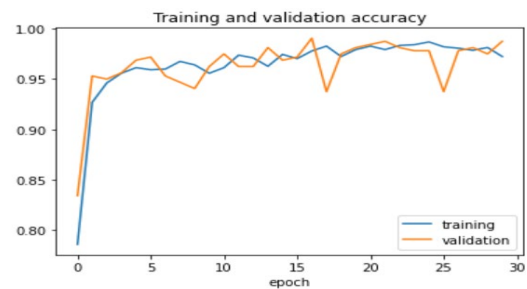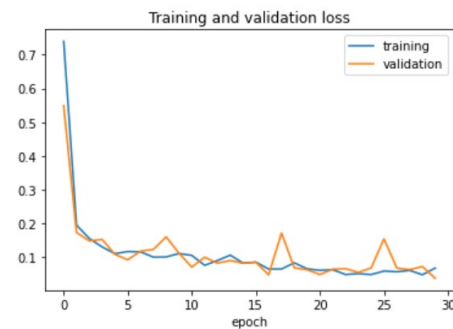| Optimization Algorithms	Validation Accuracy (%)
Adaptive Momentum	98.96
Adaptive Gradient	97.31
Adaptive Delta	96.65
RMSProp	91.51
Stochastic Gradient Descent with Momentum	86.25

Figure.10: Training vs. Validation

Figure. 11: Training vs. loss

Table 2 presents an overview of the application of the Adaptive Momentum (Adam) Optimization Algorithm, which blends principles from the Stochastic Gradient Descent with Momentum (SGDM) and RMSProp Algorithms. Figures 10 and 11 furnish visual representations showcasing the training and validation accuracy and the training and loss trends during the experimentation. These graphical depictions illustrate the refinement of weights and parameters, yielding an impressive validation accuracy of 98.96%.

Moreover, the principal aim of this Lightweight Neural Network model is to enhance performance and response time in detecting SARS-CoV-2-induced Pneumonia from Chest X-ray images. Consequently, it's pertinent to consider factors such as Time Complexity and Space Complexity. The model demonstrates remarkable swiftness in execution, requiring just 240 milliseconds for the detection process, and it maintains a minimal runtime memory footprint, occupying a mere 275 kilobytes.

In evaluating a Neural Network model's practical utility, it's imperative to account for various critical aspects. The architecture proposed within this research paper signifies a noteworthy advancement in medical science. Notably, when supplied with ample training data, the Shallow Convolution Neural Network (S-ConvNet) exhibits an enhanced capacity to learn intricate, non-linear functions, rendering it adept at distinguishing results compared to other CNN architectures. Furthermore, S-ConvNet excels in computational efficiency and input parameters, often integrating subtle features into the optimization process, contributing to its overall effectiveness.

Compared to other CNN architectures with deep representation in each layer, the architecture's optimal hidden layer design allows the input network to learn a new, more abstract input model [32]. This collective set of attributes underscores the innovation and potential of this research.

4. Future Research

This study presents a promising approach to automating the detection of SARS-COV-2-induced pneumonia from chest X-ray images. The high accuracy achieved by the proposed model has significant implications for clinical practice, particularly in resource-constrained settings. However, further research and validation are needed to fully realize the potential of this technology in improving patient care and public health efforts during the SARS-COV-2 pandemic and beyond. The utility and applicability of the Lightweight Stacked Convolutional Neural Network architecture extend beyond its initial purpose of binary detection tasks. This versatile architecture can be effectively employed for multi-class detection sce-narios, broadening its scope significantly. Beyond detecting SARS-CoV-2, standard cases, and pneumonia, it can also be adapted to identify various types of pneumonia and other medical conditions, utilizing diverse imaging modalities such as CT, mammography, ultra-sonography, and blood sample images.

Furthermore, this proposed Neural Network model is adaptable to classify different protein structure images, aiding in detecting various diseases. Its lightweight nature enables seamless deployment on standard computing devices, including personal computers and smartphones. Future research should focus on the model's robustness in real-world clinical settings, including external validation on diverse datasets. Integration with electronic health records and clinical decision support systems can enhance the model's practical utility. Moreover, ethical considerations regarding patient data privacy and regulatory approvals should be addressed when implementing such automated diagnostic tools in healthcare. To enhance the applicability of our model, future research directions may include:

- Localization Techniques: Exploring advanced computer vision techniques, such as object detection and segmentation, to precisely identify the ROI within the af-fected lung region. This would require annotated datasets that include ROI infor-mation.
- Multi-Modal Fusion: Integrating additional medical imaging modalities, such as CT scans or MRI, to complement X-ray data and provide a more comprehensive view of the infection's location and extent.
- Clinical Validation: Collaborating with medical experts and conducting clinical studies to assess the model's performance in real-world healthcare settings and its impact on diagnosis and patient care.
- Data Augmentation: Expanding the dataset with diverse and well-annotated im-ages that include ROI information, enabling the model to learn and generalize bet-ter to capture specific infection patterns.

5. Conclusion

This study represents a significant achievement in applying supervised Stacked Convolutional Neural Networks to medical science and biomedical applications. Departing from prior SARS-COV-2 research, our methodology stands out due to its unique approach, delivering exceptional accuracy while maintaining minimal Time Complexity and Memory requirements. In ongoing advancements in Deep Neural Network architectures striving for higher accuracy, our research introduces a pioneering concept by adopting a Shallow Learning paradigm with the Lightweight Stacked CNN architecture. This innovative approach achieves impressive accuracy and brings notable efficiency in response time and computational resource usage.

The streamlined Lightweight architecture we propose is crucial in expediting and enhancing the response time for SARS-COV-2 diagnosis. Given the medical nature of this research, it's essential to emphasize our unwavering commitment to ethical practices, data privacy, and the protection of patient rights. All data in this study underwent thorough anonymization and adhered to relevant data protection regulations and guidelines.

Furthermore, it's worth noting that this research received approval from the Institutional Review Board (IRB). This IRB approval assures that our research aligns with ethical standards and upholds the rights and privacy of patients. While our study presents promising results in the accurate detection of SARS-COV-2 -induced pneumonia using a lightweight stacked Convolutional Neural Network (CNN), it is essential to acknowledge the following limitations:

a. Dataset Imbalance: The dataset used in this study exhibits a significant imbalance between SARS-COV-2 cases and standard cases. While we employed

data aug-mentation techniques to address this issue, a more extensive and diverse dataset would further enhance the model's robustness.

b. Clinical Validation: Although our model shows promising results in detecting SARS-COV-2-induced pneumonia in chest X-rays, it should be validated in clini-cal settings with a broader range of patient populations and imaging equipment.

c. Interpretability: Deep learning models, including CNNs, are often considered black-box models due to their complex architecture. Ensuring model interpretabil-ity and providing insights into its decision-making process is an ongoing challenge.

d. Ethical Considerations: Deploying AI-based diagnostic tools in healthcare raises ethical concerns, such as data privacy, bias, and transparency. These aspects need careful consideration and mitigation strategies.

Addressing these limitations and further research in these areas will contribute to the refinement and broader applicability of our proposed model for SARS-COV-2 diagnosis in clinical practice.

References

[1] Xie, X., Zhong, Z., Zhao, W., Zheng, C., Wang, F., & Liu, J. (2020). Chest CT for Typi-cal Coronavirus Disease 2019 (SARS-COV-2) Pneumonia: Relationship to Negative RT-PCR Testing. Radiology, 296(2), E41-E45. https://doi.org/10.1148/radiol.2020200343

[2] Fang, Y., Zhang, H., Xie, J., Lin, M., Ying, L., Pang, P., & Ji, W. (2020). Sensitivity of Chest CT for SARS-COV-2: Comparison to RT-PCR. Radiology, 296(2), E115-E117. https://doi.org/10.1148/radiol.2020200432

[3] Eastin, C., & Eastin, T. (2020). Clinical Characteristics of Coronavirus Disease 2019 in China. The Journal Of Emergency Medicine, 58(4), 711-712. https://doi.org/10.1016/j.jemermed.2020.04.004

[4] Swapnarekha, H., Behera, H., Nayak, J., & Naik, B. (2020). Role of intelligent compu-ting in SARS-COV-2 prognosis: A state-of-the-art review. Chaos, Solitons & Frac-tals, 138, 109947. https://doi.org/10.1016/j.chaos.2020.109947

[5] Mohamadou, Y., Halidou, A., & Kapen, P. (2020). A review of mathematical modeling, artificial intelligence, and datasets used in the study, prediction, and management of SARS-COV-2. Applied Intelligence, 50(11), 3913-3925. https://doi.org/10.1007/s10489-020-01770-9

[6] Yan, T., Wong, P., Ren, H., Wang, H., Wang, J., & Li, Y. (2020). The automatic distinc-tion between SARS-COV-2 and common pneumonia using multi-scale convolutional neural network on chest CT scans. Chaos, Solitons & Fractals, 140, 110153. https://doi.org/10.1016/j.chaos.2020.110153

[7] Li, Y., Zhang, Z., Dai, C., Dong, Q., & Badrigilan, S. (2020). Accuracy of deep learning for automated detection of pneumonia using chest X-ray images: A systematic review and meta-analysis. Computers In Biology and Medicine, 123, 103898. https://doi.org/10.1016/j.compbiomed.2020.103898

[8] Elaziz, M., Hosny, K., Salah, A., Darwish, M., Lu, S., & Sahlol, A. (2020). New ma-chine learning method for image-based diagnosis of SARS-COV-2 . PLOS ONE, 15(6), e0235187. https://doi.org/10.1371/journal.pone.0235187

[9] Khandual, A., Dutta, K., Lenka, R., Nayak, S., & Bhoi, A. (2021). MED-NET: a novel approach to ECG anomaly detection using LSTM auto-encoders. International Journal Of Computer Applications In Technology, 65(4), 343. https://doi.org/10.1504/ijcat.2021.10040403

[10] Gupta, P., Saxena, N., Sharma, M., & Tripathi, J. (2018). Deep Neural Network for Human Face Recognition. International Journal Of Engineering And Manufactur-ing, 8(1), 63-71. https://doi.org/10.5815/ijem.2018.01.06

[11] Lenka, R., Dutta, K., Khandual, A., & Nayak, S. (2020). Bio-Medical Image Pro-cessing. Examining Fractal Image Processing And Analysis, 158-169. https://doi.org/10.4018/978-1-7998-0066-8.ch007

[12] Cheng, J., Ni, D., Chou, Y., Qin, J., Tiu, C., & Chang, Y. et al. (2016). Computer-Aided Diagnosis with Deep Learning Architecture: Applications to Breast Lesions in US Images and Pulmonary Nodules in CT Scans. Scientific Reports, 6(1). https://doi.org/10.1038/srep24454

[13] Reid, S., Tibshirani, R., & Friedman, J. (2016). A study of error variance estimation in Lasso regression. Statistica Sinica. https://doi.org/10.5705/ss.2014.042

[14] Hara, K., Saito, D., & Shouno, H. (2015). Analysis of function of rectified linear unit used in deep learning. 2015 International Joint Conference On Neural Networks (IJCNN). https://doi.org/10.1109/ijcnn.2015.7280578

[15] Dubey, A.K. and Jain, V. (2019). Comparative Study of Convolution Neural Network's ReLu and Leaky-ReLu Activation Functions. In Applications of Computing, Automation and Wireless Systems in Electrical Engineering Springer, pp. 873-880. https://arxiv.org/pdf/2109.14545.pdf

[16] Wanto, A., Windarto, A., Hartama, D., & Parlina, I. (2017). Use of Binary Sigmoid Function And Linear Identity In Artificial Neural Networks For Forecasting Population Density. IJISTECH (International Journal Of Information System & Technology), 1(1), 43. https://doi.org/10.30645/ijistech.v1i1.6

[17] Ramos, D., Franco-Pedroso, J., Lozano-Diez, A., & Gonzalez-Rodriguez, J. (2018). Deconstructing Cross-Entropy for Probabilistic Binary Classifiers. Entropy, 20(3), 208. https://doi.org/10.3390/e20030208

[18] Diederik, P., Kingma and Jimmy Lei Ba. (2015). Adam: A Method for Stochastic Op-timization. International Conference on Learning Representations, pp. 1-13. https://moodle2.cs.huji.ac.il/nu15/pluginfile.php/316969/mod_resource/content/1/adam_pres.pdf

[19] Boltzmann, L. (1974). The Second Law of Thermodynamics. Theoretical Physics And Philosophical

Problems, 13-32. https://doi.org/10.1007/978-94-010-2091-6_2

[20] Rowlinson *, J. (2005). The Maxwell–Boltzmann distribution. Molecular Phys-ics, 103(21-23), 2821-2828. https://doi.org/10.1080/002068970500044749

[21] Luque, A., Carrasco, A., Martín, A., & de las Heras, A. (2019). The impact of class imbalance in classification performance metrics based on the binary confusion ma-trix. Pattern Recognition, 91, 216-231. https://doi.org/10.1016/j.patcog.2019.02.023

[22] Goutte, C., & Gaussier, E. (2005). A Probabilistic Interpretation of Precision, Recall and F-Score, with Implication for Evaluation. Lecture Notes In Computer Science, 345-359. https://doi.org/10.1007/978-3-540-31865-1_25

[23] Kumar, A., Sarkar, S., & Pradhan, C. (2019). Malaria Disease Detection Using CNN Technique with SGD, RMSprop and ADAM Optimizers. Studies In Big Data, 211-230. https://doi.org/10.1007/978-3-030-33966-1_11

[24] Huk, M. (2020). Stochastic Optimization of Contextual Neural Networks with RMSprop. In Asian Conference on Intelligent Information and Database Systems Springer, Cham pp. 343-352.

[25] Chouhan, V., Singh, S., Khamparia, A., Gupta, D., Tiwari, P., & Moreira, C. et al. (2020). A Novel Transfer Learning Based Approach for Pneumonia Detection in Chest X-ray Images. Applied Sciences, 10(2), 559. https://doi.org/10.3390/app10020559

[26] Satpathy, S., Mangla, M., Sharma, N., Deshmukh, H., & Mohanty, S. (2021). Predicting mortality rate and associated risks in SARS-COV-2 patients. Spatial Information Re-search, 29(4), 455-464. https://doi.org/10.1007/s41324-021-00379-5

[27] Khadidos, A., Khadidos, A., Kannan, S., Natarajan, Y., Mohanty, S., & Tsaramirsis, G. (2020). Analysis of SARS-COV-2 Infections on a CT Image Using DeepSense Mod-el. Frontiers In Public Health, 8. https://doi.org/10.3389/fpubh.2020.599550

[28] Dutta, K., & Gupta, P. (2022, December). Reso-Net: Generic Image Resolution En-hancement Using Convolutional Autoencoders. In International Conference on Intelli-gent Systems and Machine Learning (pp. 298-308). Cham: Springer Nature Switzerland.

[29] Sah S, Surendiran B, Dhanalakshmi R, Yamin M. SARS-CoV-2 cases prediction using SARIMAX Model by tuning hyperparameter through grid search cross-validation ap-proach. Expert Syst. 2022 Jul 15:e13086. doi: 10.1111/exsy.13086.

[30] Shankar, K., Mohanty, S.N., Yadav, K. et al. Automated SARS-COV-2 diagnosis and classification using convolutional neural network with fusion based feature extraction model. Cogn Neurodyn (2021). https://doi.org/10.1007/s11571-021-09712-y

[31] Sah, S., Surendiran, B., Dhanalakshmi, R., Mohanty, S. N., Alenezi, F., & Polat, K. (2022). Forecasting SARS-COV-2 Pandemic Using Prophet, ARIMA, and Hybrid Stacked LSTM-GRU Models in India. Computational and Mathematical Methods in Medicine, 2022, 1–19. https://doi.org/10.1155/2022/1556025

[32] Shome D, Kar T, Mohanty SN, Tiwari P, Muhammad K, AlTameem A, Zhang Y, Saudagar AKJ. COVID-Transformer: Interpretable SARS-COV-2 Detection Using Vi-sion Transformer for Healthcare. Int J Environ Res Public Health. 2021 Oct 21;18(21):11086. doi: 10.3390/ijerph182111086.

[33] Gupta M., Jain R., Taneja S., Chaudhary G., Khari M. and Verdú E., Real-time meas-urement of the uncertain epidemiological appearances of SARS-COV-2 infections, Ap-plied Soft Computing, vol.101, pp.107039, 2021.

[34] Rajagopal A., Joshi G.P., Ramachandran R., Subhalakshmi R. T., Khari M., Jha S, and You J., A deep learning model based on multi-objective particle swarm optimization for scene classification in unmanned aerial vehicles, IEEE Access, vol.8, pp.135383-135393, 2020.

[35] Yousef, R., Gupta, G., Yousef, N. and Khari, M., A holistic overview of deep learning approach in medical imaging, Multimedia Systems, vol.28, Issue.3, pp.881-914, 2022.

[36] Adil Khadidos, A Robust and Computationally Faser Approach to SARS-COV-2 Diagnosis using Shallow Convolutional Neural Architecture, Paper ID: 12A13Q Volume 12 Issue 13